Improving coherence with nested environments

H. J. Moreno,[1,2] T. Gorin,[3] and T. H. Seligman[2,4]

[1] *Centro de Investigación en Ciencias, Universidad Autónoma del Estado de Morelos, Cuernavaca, Morelos, México.*
[2] *Instituto de Ciencias Físicas, Universidad Nacional Autónoma de México, Cuernavaca, México.*
[3] *Departamento de Física, Universidad de Guadalajara, Guadalajara, Jalísco, México.*
[4] *Centro Internacional de Ciencias A.C., Cuernavaca, México.*

We have in mind a register of qubits for an quantum information system, and consider its decoherence in an idealized but typical situation. Spontaneous decay and other couplings to the far environment considered as the world outside the quantum apparatus will be neglected, while couplings to quantum states within the apparatus, i.e. to a near environment are assumed to dominate. Thus the central system couples to the near environment which in turn couples to a far environment. Considering that the dynamics in the near environment is not sufficiently well known or controllable, we shall use random matrix methods to obtain analytic results. We consider a simplified situation where the central system suffers weak dephasing from the near environment, which in turn is coupled randomly to the far environment. We find the anti-intuitive result that increasing the coupling between near and far environment actually protects the central qubit.

PACS numbers: 03.65.Yz,05.45.Mt,42.50.Lc
Keywords: open quantum systems, random matrix theory, decoherence

In many quantum optics experiments and quantum information devices we find the following situation: The central system, well protected from simple decoherence processes such as spontaneous emission or direct coupling to a structureless heat bath, still suffers some decoherence from the coupling to the quantum part of the apparatus. We will call the former the far environment and the latter the near environment. In such a tripartite system without direct coupling between central system and far environment, we find that increasing the coupling of the near to the far environment can protect the central system against decoherence. In the setting of the Haroche experiment [1, 2] the late M. C. Nemes discussed this somewhat anti-intuitive fact with one of the authors [3] twelve years ago. More recently, additional numerical evidence has appeared [4], some of which were master thesis related to the present work [5–7]. Finally, it was shown in Ref. [8] that a protected subspace can appear in a strong coupling limit.

We now wish to construct a model that allows some analytical treatment and simultaneously has some claim to universality. Indeed the intermediate environment in a quantum information system typically consists of quantum states that are not used but are unavoidably present. While ordered and systematic couplings can be minimized with good technology, it is plausible that the uncontrolled remanent will have a random structure. Considering its minimum information character [9], we use random matrix theory (RMT) of decoherence [10–12]. There are several examples, which involve chaotic or irregular dynamics explicitly: *e.g.* the coupling of two-level atoms to quantum systems with classical chaotic analog [13, 14], and the experimental realization of quantum chaos in a chain of three level atoms in [15]. The recent advances in the design and control of chains of individual ions [16], may lead to similar experimental systems. We simplify the picture by limiting the coupling between central system and near environment to dephasing [17, 18], and assume the coupling between near and far environment to be of a tensor product form; see Eq. (1), below. We can then take advantage of analytic expressions that exist for dephasing in absence of the far environment [17–21] and treat the effect of the far environment within a linear response calculation. We thus obtain analytic expressions for weak couplings between near and far environment, note that this range of coupling strengths is exactly opposite to that treated in Ref. [8]. To study the effect of the far environment beyond the linear response approximation, we perform numerical simulations, using a modified Caldeira-Leggett master equation [22], whose equivalence to RMT models has first been discussed in Ref. [23].

Model: The full system consists of three parts, the central system, the near environment and the far environment with Hilbert spaces $\mathcal{H}_\mathrm{c}$, $\mathcal{H}_\mathrm{e}$ and $\mathcal{H}_\mathrm{f}$, respectively. The unitary evolution of the entire system is given by the Hamiltonian

$$H_\mathrm{tot} = H_0 + v_\mathrm{c} \otimes V_\mathrm{e} \otimes \mathbb{1}_\mathrm{f} + \gamma\, \mathbb{1}_\mathrm{c} \otimes V'_\mathrm{e} \otimes V_\mathrm{f} \qquad (1)$$

where $H_0 = h_\mathrm{c} \otimes \mathbb{1}_\mathrm{e,f} + \mathbb{1}_\mathrm{c} \otimes H_\mathrm{e} \otimes \mathbb{1}_\mathrm{f} + \mathbb{1}_\mathrm{c,e} \otimes H_\mathrm{f}$. Tracing out both environments leads to the reduced dynamics of the central system $\varrho_c(t) = \mathrm{tr}_\mathrm{e,f}[\varrho_\mathrm{tot}(t)]$, with

$$\varrho_\mathrm{tot}(t) = \exp(-\mathrm{i}H_\mathrm{tot}t/\hbar)\ \varrho_\mathrm{c} \otimes \varrho_\mathrm{e,f}\ \exp(\mathrm{i}H_\mathrm{tot}t/\hbar)\ , \qquad (2)$$

where ϱ_c and $\varrho_\mathrm{e,f}$ represent the initial states of the central system (typically assumed to be pure), and the environment (near and far environment), respectively. The couplings are given by the tensor products $v_\mathrm{c} \otimes V_\mathrm{e}$ (between central system and near environment) and $\gamma\, V'_\mathrm{e} \otimes V_\mathrm{f}$ (between near and far environment). The former will be chosen as dephasing, such that $[h_\mathrm{c}, v_\mathrm{c}] = 0$. Such couplings are frequently used, as they simplify calculations and maintain many essential properties.

Dynamics: We write the Hamiltonian as $H_{\rm tot} = \sum_j |j\rangle\langle j| \otimes H_{\rm e,f}^{(j)}$, with

$$H_{\rm e,f}^{(j)} = \big(\varepsilon_j\, \mathbb{1}_{\rm e} + H_{\rm e} + \nu_j\, V_{\rm e}\big)\otimes \mathbb{1}_{\rm f} + \mathbb{1}_{\rm e}\otimes H_{\rm f} + \gamma\, V_{\rm e}'\otimes V_{\rm f}\ , \quad (3)$$

where the set of states $\{\, |j\rangle\,\}_j$ is a common eigenbasis of $h_{\rm c}$ and $v_{\rm c}$, while ε_j and ν_j are the corresponding eigenvalues. The evolution of the whole system can be written as $\varrho_{\rm tot}(t) = \sum_{jk} \rho_{jk}(0)\, |j\rangle\langle k| \otimes \varrho^{(j,k)}(t)$, where $\varrho_{\rm c} = \sum_{jk} \rho_{jk}(0)\, |j\rangle\langle k|$ is the initial state of the central system, and

$$\varrho^{(j,k)}(t) = \exp\big(-{\rm i}H_{\rm e,f}^{(j)} t/\hbar\big)\ \varrho_{\rm e,f}\ \exp\big({\rm i}H_{\rm e,f}^{(k)} t/\hbar\big)\ . \quad (4)$$

We find for the matrix elements of the reduced state of the central system: $\rho_{jk}(t) = \rho_{jk}(0)\, {\rm tr}_{\rm e,f}[\varrho^{(j,k)}(t)]$. Since ${\rm tr}_{\rm e,f}[\varrho^{(j,j)}(t)] = 1$, the diagonal elements are constant in time, while the off-diagonal ones (i.e. the coherences) are given as expectation values of generalized echo operators in the composite environment; see Eq. (6) and Ref. [24].

In other words focussing on an individual matrix element, $\rho_{jk}(t)$, we may introduce

$$H_\lambda = H_0 + \lambda\, V_{\rm eff} = H_{\rm e} + \nu_j\, V_{\rm e}\ ,\ H_0 = H_{\rm e} + \nu_k\, V_{\rm e}\ , \quad (5)$$

such that $\lambda\, V_{\rm eff} = (\nu_j - \nu_k)\, V_{\rm e}$. This allows to connect the coherences for vanishing coupling to the far environment ($\gamma \to 0$), with fidelity amplitudes [17, 18]. Introducing the relative coherences

$$\begin{aligned} f_{\lambda,\gamma}(t) &= \frac{\rho_{jk}(t)}{\rho_{jk}(0)\, {\rm e}^{-{\rm i}(\varepsilon_j - \varepsilon_k)t/\hbar}} \\ &= {\rm tr}_{\rm e,f}\big[{\rm e}^{-{\rm i}H_{\lambda,\gamma}t/\hbar}\ \varrho_{\rm e,f}\ {\rm e}^{{\rm i}H_{0,\gamma}t/\hbar}\,\big]\ , \end{aligned} \quad (6)$$

where $H_{\lambda,\gamma} = H_\lambda \otimes \mathbb{1}_{\rm f} + \mathbb{1}_{\rm e}\otimes H_{\rm f} + \gamma\, V_{\rm e}'\otimes V_{\rm f}$, we find that $f_{\lambda,0}(t) \equiv f_\lambda(t)$ with

$$f_\lambda(t) = {\rm tr}_{\rm e}[M_\lambda(t)\, {\rm tr}_{\rm f}(\varrho_{\rm e,f})]\ , \quad M_\lambda(t) = {\rm e}^{{\rm i}H_0 t/\hbar}\, {\rm e}^{-{\rm i}H_\lambda t/\hbar}\ . \quad (7)$$

Hence, $f_{\lambda,0}(t)$ becomes the fidelity amplitude for perturbing the Hamiltonian H_0 by $\lambda\, V_{\rm eff}$, given the initial state ${\rm tr}_{\rm f}(\varrho_{\rm e,f})$ in the near environment.

Modeling the effect of the far environment, we consider the simplest possible situation, where random matrix and master equation descriptions are equivalent [23]. This will allow to use a master equation for numerics and the random matrix model for analytics. In Ref. [11], it has been shown that without central system, the coherences in the near environment decay with the rate $\Gamma = 2\pi\, N_{\rm e}\, \gamma^2/(\hbar\, d_{\rm f})$, which is just $N_{\rm e}$ times the Fermi-golden-rule rate for transitions between individual states. Here, γ^2 replaces the magnitude squared of the coupling matrix elements, since in our case $V_{\rm f}$ is chosen from a appropriately normalized random matrix ensemble, while $d_{\rm f}$ denotes the average level spacing (or inverse level density) of $H_{\rm f}$, and N_e is the dimension of the near environment. Choosing the Caldeira-Leggett master equation to describe the far environment, one obtains practically the same reduced dynamics. The only difference is that Γ then depends on the dissipation constant and the temperature [5, 6].

Linear response calculation: Applying the linear response approximation in the Fermi golden rule regime to the coupling between near and far environment (see appendix), one arrives at

$$f_{\lambda,\Gamma}(t) \sim (1 - \Gamma t)\ f_\lambda(t) + \Gamma \int_0^t {\rm d}\tau\ f_\lambda(\tau)\ f_\lambda(t-\tau)\ . \quad (8)$$

The symbol $\sim$ means equal up to $\mathcal{O}(\Gamma^2)$, and from know on, we replace γ by the physically more meaningful decoherence rate Γ. As we will see below, Eq. (8) equation is valid as long as $\Gamma t \ll 1$. It constitutes our main result. The details of its derivation can be found in the appendix. Note that the result is valid for any Hamiltonian $H_{\rm e}$, which may result in very different behaviors of $f_\lambda(t)$. The only necessary assumption is that $V_{\rm e}'$ is sufficiently random.

Generally, we find that increasing the coupling strength to the far environment is indeed slowing down the decoherence in the central system. Depending on the interaction strength between central system and near environment, and on the functional form of $f_\lambda(t)$, the effect can be more or less pronounced. This can be demonstrated for generic systems, where one often finds that $f_\lambda(t)$ changes from an exponential decay in the Fermi golden rule regime to a Gaussian decay in the perturbative regime [19, 25]. In the former the effect is zero, which can also be understood in physical terms. In that regime the temporal correlations $\langle \tilde V_{\rm eff}(t) \tilde V_{\rm eff}(t')\rangle$ of the perturbation in the interaction picture decay very fast – on a time scale $t_{\rm corr} \ll t_{\rm dec}({\rm ce})$, the decoherence time in the central system. Therefore, even if the decoherence time in the near environment $t_{\rm dec}({\rm ef}) = \Gamma^{-1}$ is smaller than $t_{\rm dec}({\rm ce})$, as long as $t_{\rm dec}({\rm ef}) > t_{\rm corr}$, the far environment will have no effect on the decoherence in the central system. In the perturbative regime by contrast, $f_\lambda(t) = {\rm e}^{-\lambda^2 t^2}$, such that $f_{\lambda,\Gamma}(t) \sim g_{\Gamma/\lambda}(\lambda t)$ with

$$g_\alpha(x) = (1 - \alpha\, x)\ {\rm e}^{-x^2} + \alpha\ \sqrt{\pi/2}\ {\rm e}^{-x^2/2}\ {\rm erf}\big(x/\sqrt{2}\big)\ . \quad (9)$$

Although exact analytical results for $f_\lambda(t)$ exist [20, 21], for simplicity, we will compare our results to the exponentiated linear response (ELR) expression from Ref. [19].

$$\begin{aligned} f_\lambda^{\rm ELR}(t) &= \exp[-\lambda^2\, C(t)\,] \quad (10) \\ C(t) &= t^2 + \pi\, t - 4\pi^2 \int_0^{t/(2\pi)} {\rm d}t' \int_0^{t'} {\rm d}t''\ b_2(t'')\ , \end{aligned}$$

where $b_2(t)$ is the two-point form factor [26].

Caldeira-Leggett master equation: For full-fledged numerical random matrix calculations, we would need to work in the Hilbert space of near and far environment. For the far environment, we would need a smaller mean level spacing in combination with a larger spectral span, as compared to the near environment. Still, in order to

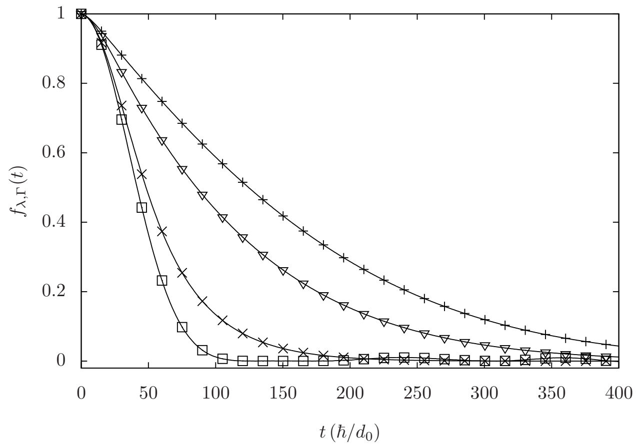

FIG. 1. Relative coherence $f_{\lambda,\Gamma}(t)$ in the Caldeira-Leggett model in the perturbative regime ($\lambda = 0.02$), for different values of the coupling to the heat bath: $\Gamma/\lambda = 0$ (squares), 1.0 (shaped crosses), 5.0 (inverted triangles) and 10.0 (crosses). The time is in units of $\hbar/d_0$ where $2\pi\hbar/d_0$ is the Heisenberg time and d_0 the mean level spacing in the near environment. In all cases $N_{\rm e} = 50$ and $n_{\rm run} = 1\,000$ realizations.

justify the use of RMT, we would need as many levels as possible also in the near environment. Such random matrix calculations are not viable, due to the dimension of the Hamiltonian matrices involved.

We will therefore use an approach which allows to work in the Hilbert space of the near environment alone, taking the effect of the far environment into account via the Caldeira-Leggett master equation [22], where we replace the diagonal matrix representation of the harmonic oscillator Hamiltonian with a random matrix, defined as in Eq. (5). We choose both matrices H_0 and $V_{\rm eff}$ from the Gaussian orthogonal ensemble (GOE). We scale H_0 in such a way that the mean level spacing becomes one in the center of the spectrum. The matrix elements of $V_{\rm eff}$ are chosen to have the variances $\langle V_{ij}^{{\rm eff}\,2}\rangle = 1 + \delta_{ij}$. In that way, the strength of the perturbation (implied by the dephasing coupling to the central system), measured in units of the mean level spacing d_0, is given by λ. In the following figures we scale time by the Heisenberg time $t_{\rm H} = 2\pi\hbar/d_0$.

Numerical simulations: The use of random matrices requires a Monte Carlo average over many realizations. As a sufficiently large but still numerically manageable dimension of the environment, we choose $N_{\rm e} = 50$, and perform averages over $n_{\rm run} = 1\,000$ realisations. The general behaviour of the relative coherence $f_{\lambda,\Gamma}(t)$ is shown in Fig. 1. Here, we choose $\lambda = 0.02$ for the dephasing coupling, and different values for the coupling strength Γ between both environments. The figure clearly shows that the coherence decays slower by increasing Γ.

In the remaining figures, we evaluate the quality of our analytical result from Eq. (8). For a better quantitative comparison, we subtract the ELR approximation

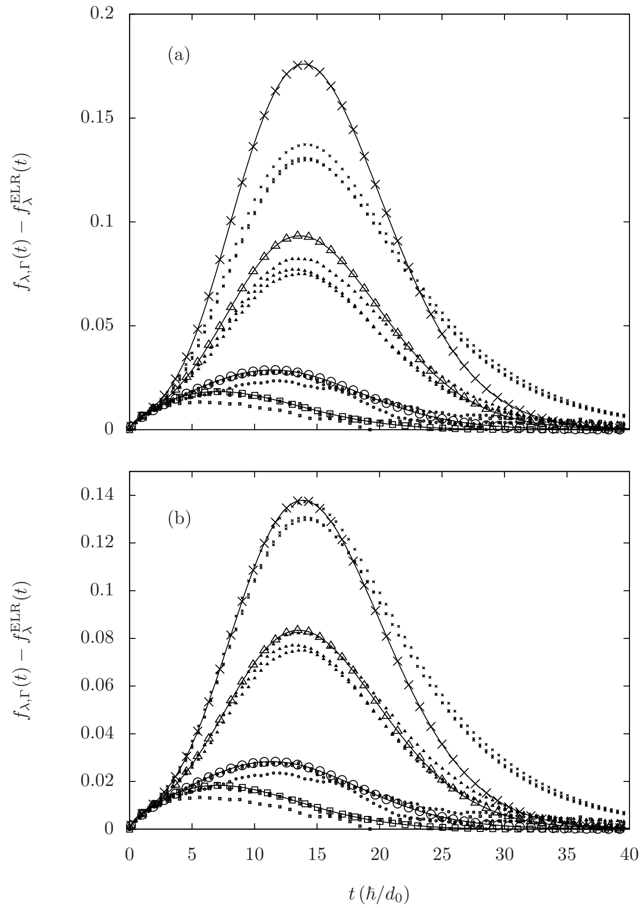

FIG. 2. (a) Relative coherence $f_{\lambda,\Gamma}(t)$ subtracted by the exponentiated linear response approximation $f_\lambda^{\rm ELR}(t)$ to the fidelity amplitude, for $\lambda = 0.1$ (cross-over regime) and different values for the coupling to the heat bath: $\Gamma/\lambda = 0$ (squares), 0.1 (circles), 0.5 (triangles), and 1.0 (shaped crosses). The thick solid lines, show the analytical result according to Eq. (8), and the nearest thin dotted lines show three statistically independent ensemble averages for each case. (b) The same quantity as in panel (a), but for the theoretical curves the values for Γ are replaced by best fit values $\Gamma_{\rm fit}$ such that: $\Gamma_{\rm fit}/\lambda = 0.097$ (circles), 0.44 (triangles), and 0.77 (shaped crosses), obtained for the region $0 < t < 15$. The units of time are the same as in Fig 1.

$f_\lambda^{\rm ELR}(t)$ for pure fidelity decay, from both, the numerical simulation and the analytical approximation for $f_{\lambda,\Gamma}(t)$. Note that for the function $f_\lambda(t)$ appearing in the analytical expression, we use numerical results with much improved accuracy. These are obtained from numerical simulations without far environment and some subsequent spline-fitting for facilitating the evaluation of the integral in Eq. (8). In that way, the accuracy can be greatly improved. The numerical result for $f_{\lambda,0}(t)$ differs from the ELR result due to the fact that $f_\lambda^{\rm ELR}(t)$ is only an approximation, but also because of the level density over the spectral range of H_0. The remaining difference to the exact analytical expression found by Stöckmann

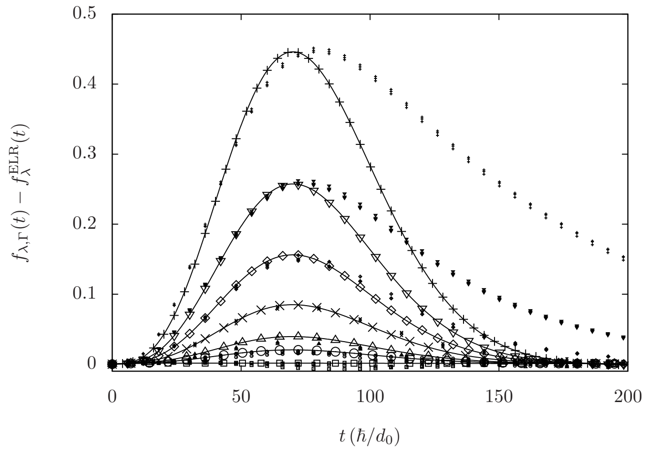

FIG. 3. Comparison between Caldeira-Leggett simulations and the linear response theory as in Fig. 2, but for $\lambda = 0.02$. The units of time are the same as in Fig 1. For the theoretical curves, we rescaled $\Gamma_{\rm fit}$ as explained in the text. The different cases shown are: (squares) $\Gamma = 0$, circles $\Gamma(\Gamma_{\rm fit}) = 0.002$ (0.00195), triangles 0.004 (0.0039), shaped crosses 0.01 (0.00858), diamonds 0.02 (0.0159), inverted triangles 0.04 (0.0263), crosses 0.1 (0.0457).

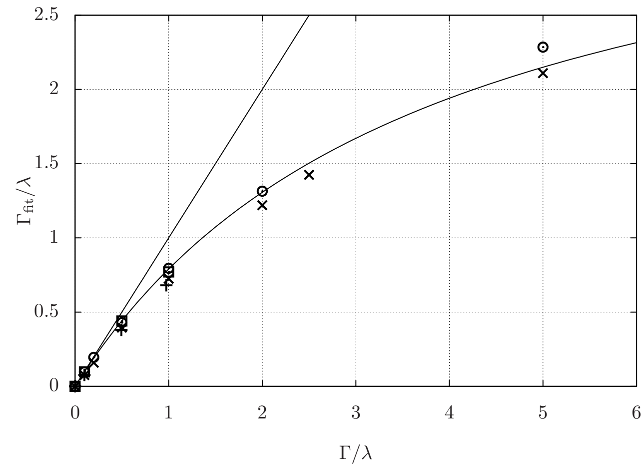

FIG. 4. $\Gamma_{\rm fit}/\lambda$ vs. Γ/λ for $\lambda = 0.1$, $N_{\rm e} = 25$ and $N_{\rm e} = 50$ (crosses and squares respectively) and $\lambda = 0.02$, $N_{\rm e} = 25$ (shaped crosses). The solid lines show the functions $\Gamma_{\rm fit}/\lambda = \alpha$ and $b\,\alpha/(b+\alpha)$ with $b = 3.77$ and $\alpha = \Gamma/\lambda$.

and Schäfer [20, 21], is due to the fact that the trace in Eq. (7) includes the full spectral range where the level density varies according to the semi-circle law.

In Fig. 2(a) we consider the case $\lambda = 0.1$, which is in the cross-over regime. Since we are plotting the difference $f_{\lambda,\Gamma}(t) - f_\lambda^{\rm ELR}(t)$, the stabilizing effect of the far environment shows up as a growing positive hump. For each value of Γ, we plot three statistically independent numerical simulations. This gives us an idea about the statistical uncertainty of the results. We can clearly see that the curves which correspond to $\Gamma = 0$ are different from zero, due to the reasons discussed. Additional cases with increasing coupling to the heat bath. For those cases, the relative coupling strength Γ/λ is 0.1 (circles), 0.5 (triangles), and 1.0 (shaped crosses). We can observe that the theory agrees with the simulations, only in the case of smallest coupling, for stronger coupling the effect is systematically overestimated. In Fig. 2(b) we intend to find a rescaled decoherence rate $\Gamma_{\rm fit}$, which best describes the numerical results, and hence the stabilizing effect of the far environment on the central system. A good agreement could be achieved only for times up to $t_{\max} \approx 15$, which is the approximate location of the maxima of the curves shown.

In Fig. 3 we repeat the comparison for $\lambda = 0.02$, where the coupling between central system and RMT environment is close to the perturbative regime. We use the same fitting procedure as in Fig. 2(b). Here, the values for the relative coupling strength Γ/λ range from 0.1 to 5.0. The slowing down of decoherence in the central system due to the increasing coupling to the far environment, occurs just as in the case $\lambda = 0.1$. However, for large values of Γ/λ the deviations between simulations and theory become quite noticeable, even if we use the best fit values $\Gamma_{\rm fit}$ for the theory.

Finally, we compare in Fig. 4 the fitted values $\Gamma_{\rm fit}$ for the coupling to the far environment, with the nominal ones, by plotting $\Gamma_{\rm fit}/\lambda$ versus Γ/λ. This is done for different dimensions of the near environment, for different coupling strengths between central system and near environment, and different couplings to the far environment. The derivation of our theoretical result within linear response theory showed that the deviation from the exact result should be quadratic in Γ. The results for $\Gamma_{\rm fit}/\lambda$ shown here, confirm this expectation, as they approach the line $\Gamma_{\rm fit}/\lambda = \Gamma/\lambda$ for sufficiently small values. For larger values of Γ, the fitted values for $\Gamma_{\rm fit}$, and thereby the stabilizing effect of the far environment, increase ever more slowly. To illustrate this behavior, we plotted the straight line $\Gamma_{\rm fit}/\lambda = \alpha$ as well as the function $g(\alpha) = b\,\alpha/(b+\alpha)$, with $\alpha = \Gamma/\lambda$ and a best fit value $b = 3.77$, which describes the overall behavior of the points quite well.

Summarizing, we have been able to obtain an analytic expression confirming that nested environments can improve coherence of a central system as the coupling between near and far environment increases, as long as this coupling is small. We also extended previous limited numerical evidence for large coupling using a Caldeira-Leggett master equation which has been derived from RMT considerations in previous work [6]. This confirms that the effect subsists at large couplings between near and far environment, but subsides if the central system is strongly coupled to the near environment. An explanation on the basis of the quantum Zeno effect is tempting but problematic, at least in as far as we consider weak couplings between near and far environment.

ACKNOWLEDGMENTS

We thank P. Zanardi, L. Campos Venuti, C. Gonzalez, and C. Pineda for enlightening discussions, and we acknowledge the hospitality of the Centro Internacional de Ciencias, UNAM, where many of these discussions took place. We also acknowledge financial support from CONACyT through the grants CB-2009/129309 and 154586 as well as UNAM/DGAPA/PAPIIT IG 101113.

Appendix: Derivation of the main result (Eq. 8)

1. Dephasing coupling

Under dephasing coupling, the nondiagonal element of the qubit reduced state is just the fidelity amplitude of the RMT-environment with respect to the perturbation induced by the coupling between central system and near environment. For an initial state $\varrho_{\rm e,f}$, and with $V_{\rm e,f} = V'_{\rm e} \otimes V_{\rm f}$ and $H_\lambda = H_0 + \lambda\, V_{\rm eff}$ from Eq. (5) of the main article,

$$\begin{aligned} f_{\lambda,\gamma}(t) &= {\rm tr}\big[\, \varrho_{\rm e,f}\; {\rm e}^{{\rm i}(H_0+H_{\rm f}+\gamma\, V_{\rm e,f})t/\hbar}\; {\rm e}^{-{\rm i}(H_\lambda+H_{\rm f}+\gamma\, V_{\rm e,f})t/\hbar}\,\big] \\ &= {\rm tr}\big\{\, \big[\, {\rm e}^{{\rm i}(H_\lambda+H_{\rm f})t/\hbar}\; {\rm e}^{-{\rm i}(H_\lambda+H_{\rm f}+\gamma\, V_{\rm e,f})t/\hbar}\; \varrho_{\rm e,f}\; {\rm e}^{{\rm i}(H_0+H_{\rm f}+\gamma\, V_{\rm e,f})t/\hbar}\; {\rm e}^{-{\rm i}(H_0+H_{\rm f})t/\hbar}\,\big]\; {\rm e}^{{\rm i}(H_0+H_{\rm f})t/\hbar}\; {\rm e}^{-{\rm i}(H_\lambda+H_{\rm f})t/\hbar}\,\big\}\; . \end{aligned} \tag{A.1}$$

The later two evolution operators are separable and therefore simplify as follows:

$$\begin{aligned} {\rm e}^{{\rm i}(H_0+H_{\rm f})t/\hbar}\; {\rm e}^{-{\rm i}(H_\lambda+H_{\rm f})t/\hbar} &= {\rm e}^{{\rm i}H_0\, t/\hbar} \otimes {\rm e}^{{\rm i}H_{\rm f} t/\hbar}\;\; {\rm e}^{-{\rm i}H_\lambda t/\hbar} \otimes {\rm e}^{-{\rm i}H_{\rm f} t/\hbar} \\ &= M_\lambda(t) \otimes \mathbb{1}_{\rm f}\; , \qquad M_\lambda(t) = {\rm e}^{{\rm i}H_0\, t/\hbar}\; {\rm e}^{-{\rm i}H_\lambda t/\hbar}\; . \end{aligned}$$

Since ${\rm tr}_{\rm f}[A\, M \otimes \mathbb{1}_{\rm f}] = A_{ij,kl}\; M_{km} \delta_{lj} = {\rm tr}_{\rm f}(A)\, M$ then

$$f_{\lambda,\gamma}(t) = {\rm tr}_{\rm e}\big[\, \tilde\varrho_{\rm e}(t)\; M_\lambda(t)\,\big], \quad \tilde\varrho_{\rm e}(t) = {\rm tr}_{\rm f}\big[\, {\rm e}^{{\rm i}(H_\lambda+H_{\rm f})t/\hbar}\; {\rm e}^{-{\rm i}(H_\lambda+H_{\rm f}+\gamma\, V_{\rm e,f})t/\hbar}\; \varrho_{\rm e,f}\; {\rm e}^{{\rm i}(H_0+H_{\rm f}+\gamma\, V_{\rm e,f})t/\hbar}\; {\rm e}^{-{\rm i}(H_0+H_{\rm f})t/\hbar}\,\big]\; . \tag{A.2}$$

2. Linear response approximation for the coupling to the far environment

The trace over the far environment in Eq. (A.2) is almost exactly of the form as the reduced density matrix (in the interaction picture) treated [11], namely with $\mathcal{M}_{\lambda,\gamma}(t) = {\rm e}^{{\rm i}(H_\lambda+H_{\rm f})t/\hbar}\; {\rm e}^{-{\rm i}(H_\lambda+H_{\rm f}+\gamma V_{\rm e,f})t/\hbar}$, we may write

$$f_{\lambda,\gamma}(t) = {\rm tr}_{\rm e}\big[\, \tilde\varrho_{\rm e}(t)\; M_\lambda(t)\,\big]\; , \qquad \tilde\varrho_{\rm e}(t) = {\rm tr}_{\rm f}\big[\, \mathcal{M}_{\lambda,\gamma}(t)\; \varrho_{e,f}\; \mathcal{M}_{0,\gamma}(t)^\dagger\,\big]\; . \tag{A.3}$$

However, in order to apply the formalism of [11], we should assume the coupling $V_{\rm e,f}$ and the initial state $\varrho_{\rm e,f}$ to be separable:

$$\varrho_{\rm e,f} = \varrho_{\rm e} \otimes \varrho_{\rm f}\; , \qquad V_{\rm e,f} = V'_{\rm e} \otimes V_{\rm f}\; ,$$

and:

$$\tilde V_{\rm e,f}(\tau) = \tilde v_\lambda(\tau) \otimes \tilde V_{\rm f}(\tau) = {\rm e}^{{\rm i}(H_\lambda+H_{\rm f})t/\hbar}\; V'_{\rm e} \otimes V_{\rm f}\; {\rm e}^{-{\rm i}(H_\lambda+H_{\rm f})t/\hbar}\; , \qquad \tilde v_\lambda(\tau) = {\rm e}^{{\rm i}\, H_\lambda t/\hbar}\; V'_{\rm e}\; {\rm e}^{-{\rm i}\, H_\lambda t/\hbar}\; ,$$

where we have already defined the representation $\tilde V_{\rm e,f}(t)$ of the coupling operator to the far environment in the interaction picture and similarly for $\tilde V_{\rm f}(\tau)$. Of course there remains the very important difference, that here we have different echo operators on the left and the right side of the initial state. Nevertheless, following carefully the calculation in [11], developing the echo operators into their respective Dyson series we find:

$$\begin{aligned} &\tilde\varrho_e(t) = \varrho_{\rm e} - \frac{\gamma^2}{\hbar^2}(A_J - A_I)\; , \qquad A_J = {\rm tr}_{\rm f}\big[\, J_\lambda(t)\, \varrho_{\rm e,f} + \varrho_{\rm e,f}\; J_0(t)^\dagger\,\big]\; , \quad A_I = {\rm tr}_{\rm f}\big[\, I_\lambda(t)\; \varrho_{\rm e,f}\; I_0(t)^\dagger\,\big] \\ &J_\lambda(t) = \int_0^t {\rm d}\tau \int_0^\tau {\rm d}\tau'\; \tilde V_{\rm e,f}(\tau)\, \tilde V_{\rm e,f}(\tau')\; , \qquad I_\lambda(t) = \int_0^t {\rm d}\tau\; \tilde V_{\rm e,f}(\tau)\; . \end{aligned} \tag{A.4}$$

The calculation for the average over $J_\lambda(t)$ with respect to the random matrix $V_{\rm f}$ yields

$$\langle J_\lambda(t)\rangle = \int_0^t {\rm d}\tau \int_0^\tau {\rm d}\tau'\; c(\tau-\tau')\; \tilde v_\lambda(\tau)\; \tilde v_\lambda(\tau') \otimes \mathbb{1}_{\rm f}\;, \tag{A.5}$$

where $c(\tau)$ describes the spectral correlations of $H_{\rm f}$ and β is the Dyson parameter, such that for a GUE ($\beta = 2$) or a GOE ($\beta = 1$) with Heisenberg time $\tau_{\rm H} = 2\pi\hbar/d_0$: $c(\tau) = 3 - \beta + \delta(\tau/\tau_{\rm H}) - b_2(\tau/\tau_{\rm H})$. Similarly for A_I:

$$\langle A_I\rangle = \iint_0^t {\rm d}\tau{\rm d}\tau'\; c(\tau-\tau')\; \tilde v_\lambda(\tau)\; \varrho_{\rm e}\; \tilde v_0(\tau')\;. \tag{A.6}$$

Finally, we obtain

$$\langle A_J - A_I\rangle = \int_0^t {\rm d}\tau \int_0^\tau {\rm d}\tau'\; c(\tau-\tau')\; \big\{\, \tilde v_\lambda(\tau)\, \big[\, \tilde v_\lambda(\tau')\, \varrho_{\rm e} - \varrho_{\rm e}\, \tilde v_0(\tau')\,\big] - \big[\, \tilde v_\lambda(\tau')\, \varrho_{\rm e} - \varrho_{\rm e}\, \tilde v_0(\tau')\,\big]\, \tilde v_0(\tau)\,\big\} \tag{A.7}$$

3. Fermi golden rule regime and master equation

If we assume that the Heisenberg time of the far environment $\tau_{\rm H}$ is very large, and that we are in the Fermi golden rule regime for the coupling to the far environment, then from the correlation function $c(\tau)$, we only need to take the delta function into account. That reduces Eq. (A.7) to

$$\langle A_J - A_I\rangle = \frac{\tau_H}{2} \int_0^t {\rm d}\tau\, \big[\, \tilde v_\lambda(\tau)\, \tilde v_\lambda(\tau)\, \varrho_{\rm e} - 2\, \tilde v_\lambda(\tau)\, \varrho_{\rm e}\, \tilde v_0(\tau) + \varrho_{\rm e}\, \tilde v_0(\tau)\, \tilde v_0(\tau)\,\big] \tag{A.8}$$

Next, we will average that expression over the coupling matrix $v_{\rm e}$, which is the near environment part of the coupling between near and far environment. Since this matrix is assumed to be an element of the GUE, we find:

$$\langle v_{\rm e}^2\rangle_{ik} = \sum_j v_{ij}\, v_{jk} = N_{\rm e}\, \delta_{ik} \quad\Rightarrow\quad \langle \tilde v_\lambda(\tau)\, \tilde v_\lambda(\tau)\rangle = N_{\rm e}\, \mathbb{1}_{\rm e} \tag{A.9}$$

On the other hand, we find

$$\begin{aligned}\langle \tilde v_\lambda(\tau)\, \varrho_{\rm e}\, \tilde v_0(\tau)\rangle_{iq} &= (u_\lambda^\dagger)_{ij}\, (v_{\rm e})_{jk}\, (u_\lambda)_{kl}\, \varrho^{\rm e}_{lm}\, (u_0^\dagger)_{mn}\, (v_{\rm e})_{np}\, (u_0)_{pq} \\ &= (u_\lambda^\dagger)_{ij}\, \delta_{kn}\, \delta_{jp}\, (u_\lambda)_{kl}\, \varrho^{\rm e}_{lm}\, (u_0^\dagger)_{mn}\, (u_0)_{pq} = (u_\lambda^\dagger)_{ij}\, (u_\lambda)_{kl}\, \varrho^{\rm e}_{lm}\, (u_0^\dagger)_{mk}\, (u_0)_{jq}\;,\end{aligned} \tag{A.10}$$

where $u_\lambda = \exp(-iH_\lambda t)$. This can be written as

$$\langle \tilde v_\lambda(\tau)\, \varrho_{\rm e}\, \tilde v_0(\tau)\rangle_{iq} = [M_\lambda(\tau)^\dagger]_{iq}\; {\rm tr}\big[\, \varrho_{\rm e}\, M_\lambda(\tau)\,\big] \quad \text{since} \quad M_\lambda(\tau) = u_0^\dagger\, u_\lambda\;. \tag{A.11}$$

Therefore, we obtain for $\varrho_e(t)$

$$\varrho_e(t) = \varrho_{\rm e} - \frac{\gamma^2\, \tau_H}{2\hbar^2} \left(2\, N_{\rm e}\, t\; \varrho_{\rm e} - 2 \int_0^t {\rm d}\tau\; {\rm tr}\big[\, \varrho_{\rm e}\, M_\lambda(\tau)\,\big]\; M_\lambda(\tau)^\dagger \right) \tag{A.12}$$

Let us denote $\Gamma = 2\pi\, N_{\rm e}\, \gamma^2/(\hbar d_{\rm f})$, where we introduced the average level spacing $d_{\rm f} = h/\tau_H$. Then we obtain for the fidelity amplitude:

$$f_{\lambda,\Gamma}(t) = {\rm tr}\Big[\, (1-\Gamma\, t)\; \varrho_{\rm e}\; M_\lambda(t) + \frac{\Gamma}{N_{\rm e}} \int_0^t {\rm d}\tau\; {\rm tr}\big[\, \varrho_{\rm e}\, M_\lambda(\tau)\,\big]\; M_\lambda(\tau)^\dagger\; M_\lambda(t)\,\Big] \tag{A.13}$$

thus

$$f_{\lambda,\Gamma}(t) \sim (1-\Gamma\, t)\; f_\lambda(t) + \Gamma \int_0^t {\rm d}\tau\; f_\lambda(\tau)\; f_\lambda(t-\tau) \tag{A.14}$$

where we have used that $f_\lambda(t) = {\rm tr}[\varrho_{\rm e}\, M_\lambda(\tau)]$ and $N_{\rm e}\, f_\lambda(t-\tau) = {\rm tr}[M_\lambda(t-\tau)]$. So $f_\lambda(t)$ denotes the fidelity amplitude in the near environment, if there is no coupling to the far environment ($\gamma = 0$). The first line is exact (in the limit $\Gamma t \ll 1$), assuming that no ensemble averaging has been applied with respect to $H_{\rm e}$ and $V_{\rm e}$. The second line assumes

self averaging for the quantities $\mathrm{tr}[\varrho_{\mathrm{e}}\, M_\lambda(\tau)]$ and $\mathrm{tr}[M_\lambda(t-\tau)]$ which will probably hold for generic initial states ϱ_{e} and sufficiently large near environment ($N_{\mathrm{e}} \gg 1$).

[1] M. Brune, E. Hagley, J. Dreyer, X. Maître, A. Maali, C. Wunderlich, J. M. Raimond, and S. Haroche, Phys. Rev. Lett. **77**, 4887 (1996)

[2] J. M. Raimond, M. Brune, and S. Haroche, Phys. Rev. Lett. **79**, 1964 (1997)

[3] M. C. Nemes, (private communication).

[4] E. Villaseñor, C. Gonzalez, C. Pineda, and T. H. Seligman, (unpublished)

[5] J. Castillo, Master's thesis, Universidad de Guadalajara (2011).

[6] H. J. Moreno, Master's thesis, Universidad de Guadalajara (2013).

[7] C. A. González, Master's thesis, Universidad Nacional Autonoma de México (2014).

[8] P. Zanardi and L. Campos Venuti, Phys. Rev. Lett. **113**, 240406 (2014)

[9] R. Balian, Nuovo Cimento **B 57**, 183 (1968)

[10] C. Pineda, T. Gorin, and T. H. Seligman, New J. Phys. **9**, 106 (2007)

[11] T. Gorin, C. Pineda, H. Kohler, and T. H. Seligman, New J. Phys. **10**, 115016 (2008)

[12] M. Carrera, T. Gorin, and T. H. Seligman, Phys. Rev. A **90**, 022107 (2014).

[13] F. Haug, M. Bienert, W. P. Schleich, T. H. Seligman, and M. G. Raizen, Phys. Rev. A **71**, 043803 (2005)

[14] S. Wu, A. Tonyushkin, and M. G. Prentiss, Phys. Rev. Lett. **103**, 034101 (2009)

[15] T. Graß, B. Juliá-Díaz, M. Kuś, and M. Lewenstein, Phys. Rev. Lett. **111**, 090404 (2013)

[16] T. Pruttivarasin, M. Ramm, I. Talukdar, A. Kreuter, and H. Häffner, New J. Phys. **13**, 075012 (2011)

[17] S. A. Gardiner, J. I. Cirac, and P. Zoller, Phys. Rev. Lett. **79**, 4790 (1997)

[18] T. Gorin, T. Prosen, T. H. Seligman, and W. T. Strunz, Phys. Rev. A **70**, 042105 (2004)

[19] T. Gorin, T. Prosen, and T. H. Seligman, New J. of Phys. **6**, 20 (2004)

[20] H.-J. Stöckmann and R. Schäfer, New J. Phys. **6**, 199 (2004)

[21] H.-J. Stöckmann and R. Schäfer, Phys. Rev. Lett. **94**, 244101 (2005)

[22] A. O. Caldeira and A. J. Leggett, Physica **121A**, 587 (1983)

[23] E. Lutz and H. A. Weidenmüller, Physica A **267**, 354 (1999)

[24] T. Gorin, T. Prosen, T. H. Seligman, and M. Žnidarič, Phys. Rep. **435**, 33 (2006)

[25] N. R. Cerruti and S. Tomsovic, Phys. Rev. Lett. **88**, 054103 (2002)

[26] M. L. Mehta, *Random matrices and the statistical theory of energy levels, 3rd Edition* (Academic Press, New York, 2004)